



HAL
open science

Impact of a CO₂-Enriched Gas on the Decarbonation of CaCO₃ and the Oxidation of Carbon in the Smoldering Process of Oil Shale Semicoke

M. Sennoune, Sylvain Salvador, Gérald Debenest

► **To cite this version:**

M. Sennoune, Sylvain Salvador, Gérald Debenest. Impact of a CO₂-Enriched Gas on the Decarbonation of CaCO₃ and the Oxidation of Carbon in the Smoldering Process of Oil Shale Semicoke. *Energy & Fuels*, 2012, 26 (1), pp.391-399. 10.1021/ef201304n . hal-01688406

HAL Id: hal-01688406

<https://hal.science/hal-01688406>

Submitted on 23 Mar 2018

HAL is a multi-disciplinary open access archive for the deposit and dissemination of scientific research documents, whether they are published or not. The documents may come from teaching and research institutions in France or abroad, or from public or private research centers.

L'archive ouverte pluridisciplinaire **HAL**, est destinée au dépôt et à la diffusion de documents scientifiques de niveau recherche, publiés ou non, émanant des établissements d'enseignement et de recherche français ou étrangers, des laboratoires publics ou privés.

Impact of a CO₂-Enriched Gas on the Decarbonation of CaCO₃ and the Oxidation of Carbon in the Smoldering Process of Oil Shale Semicoke

M. Sennoune,^{*,†} S. Salvador,[†] and G. Debenest[‡]

[†]Université de Toulouse, Mines Albi, Centre National de la Recherche Scientifique (CNRS), Centre RAPSODEE, Campus Jarlard, F-81013 Albi CT Cedex 09, France

[‡]Université de Toulouse, Centre National de la Recherche Scientifique (CNRS), IMFT, Allée Camille Soula, F-31400 Toulouse, France

ABSTRACT: One way of recovering oil is to propagate a co-current feed smoldering front in oil shale. This can be performed either *in situ* or as an *ex situ* process. Smoldering in oil shale semicoke achieves both thermal valorization and carbon release. In both cases, two phenomena cause CO₂ formation and release: the oxidation of fixed carbon and the decarbonation of CaCO₃. It is shown in this work that enriching the gas fed to the front with CO₂ significantly impacts both phenomena, potentially in a positive way: (i) the oxidation of fixed carbon to CO is encouraged, leading to the production of a richer gas and limiting the amount of CO₂ formed, and (ii) the decarbonation of CaCO₃ is limited, which also contributes to reducing the formation of CO₂.

1. INTRODUCTION

Smoldering combustion can be encountered in many cases, both naturally and in industry. Energy,^{1,2} environment science,^{3,4} and forest management^{5,6} have stimulated considerable research in the past few years. Previous studies consider smoldering as a complex phenomenon encompassing a number of fundamental processes, including heat and mass transfer in a porous medium, endothermic pyrolysis of combustible material, and ignition, propagation, and extinction of heterogeneous exothermic reactions at the solid–gas pore interface.

Ohlemiller⁷ defines smoldering as a slow, low-temperature, flameless form of combustion, sustained by the heat provided when oxygen directly attacks the surface of a condensed fuel (i.e. solid or liquid). Smoldering is limited by the rate of oxygen transport to the fuel surface, resulting in a slower and lower temperature reaction than that which occurs with flaming. Smoldering can be self-sustaining (i.e., no energy input is required after ignition) when the fuel is (or is embedded in) a porous medium. Self-sustaining smoldering occurs because the solid acts as an energy sink and then feeds that energy back into the unburnt fuel, creating a reaction that is highly energy-efficient.⁸

1.1. Smoldering in Oil Shale (OS) and Semicoke (SC). Smoldering is a way to recover the organic matter contained in OS in the form of oil, either *in situ* or *ex situ*. The oil recovered can be used as a petroleum-like liquid. Moreover, the flue gas that is produced may prove to be a useful source of energy.

Today, the primary solid byproduct of OS retorting is called SC. SC is the main problem of the OS industry. It is considered as a dangerous waste, which may contain pollutants including sulfates, heavy metals, and polycyclic aromatic hydrocarbons, some of which are toxic and carcinogenic.⁹ In certain countries, a large quantity of SC (about 300 million tons in Estonia, for example) is mostly placed into open dumps. The combustion of SC, as discussed in several papers,^{10,11} could be a promising concept, allowing for the use of the high residual energetic potential of this material. One drawback of this technology is that, at high temperatures, the mineral matter, mainly CaCO₃, is decarbonated, and enormous emissions of CO₂ are released. More recently,

several authors^{12,13} have proposed the use of SC ash, which contains free CaO and MgO, as a sorbent for CO₂ mineral sequestration.

1.2. Thermochemical Mechanisms Involved in SC Smoldering. Recently, Martins et al.¹⁴ carried out forward smoldering experiments in an OS porous medium and proposed a quite detailed description of the different zones involved during the propagation of the smoldering front. Four reaction zones, which propagate throughout the OS porous medium, were identified. (i) The water evaporation zone: this mechanism was assumed to be very fast and completed rapidly when the temperature reaches 150 °C. (ii) The devolatilization zone is where the temperature reaches high values (250–550 °C) allowing for the cracking of organic matter within the grains. This cracking produces gaseous species (light hydrocarbons), heavy oil, and a reactive residue called fixed carbon (FC). The devolatilization process is endothermic.¹⁵ In this zone, part of the organic matter is oxidized simultaneously. This oxidation is called low-temperature oxidation (LTO). (iii) The reaction zone is where the temperature is higher (more than 550 °C) and where oxygen carried by the fluid meets the carbon residue (FC) left by devolatilization. This exothermic oxidation reaction consumes oxygen and produces carbon monoxide and carbon dioxide. (iv) The CaCO₃ decarbonation zone (temperature above 750 °C) is possibly located in the same area as the reaction zone according to ref 15.

With the air flow rate used in experiments, the reaction leading structure prevails during the front propagation. In this situation, most of the heat released at FC oxidation is left behind the reaction zone and only a thin layer is heated downstream of the front, as illustrated further in the paper (Figure 6). Therefore, the propagation of the four reaction zones can be considered as a steady process.

1.3. Literature on Carbon Oxidation. Carbon undoubtedly plays an important role in many smoldering processes: the

self-heating evident in smoldering is a consequence of the heat generated during carbon oxidation. Oxidation occurs when the oxygen in the flowing gas comes into contact with carbon. Classically, in the case of heterogeneous reactions in a porous medium, the macro-scale rate of oxidation is controlled in some cases by the kinetics of the reactions involved and, at other times, the intra-granular diffusion of the O₂ reactant. The oxidation of carbon has been studied by many investigators (more recently in ref 16). In general, it undergoes a series of intermediate reactions, and consequently, the products CO and CO₂ are formed on the carbon surface.^{17,18} Although CO has commonly been accepted as the primary product of heterogeneous char oxidation, experimental studies have indicated that some CO₂ is also formed.¹⁹ Globally, the combustion mainly produces CO₂ and moderate amounts of CO. This partitioning between CO and CO₂ is significant (i) because of the large difference in reaction heat, which is over 3 times larger for CO₂ formation than for the CO formation reaction and (ii) in terms of the stoichiometry. A given quantity of oxygen will consume twice as much carbon if CO is produced as it will when CO₂ is produced. This will impact the reaction front velocity in the same ratio.

Determination of the ratio of produced CO/CO₂ requires a mechanism for the formation of CO and CO₂. It is well-known that the following reactions occur on the surface of a burning carbon particle:

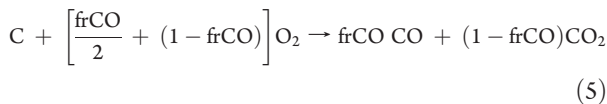


and, in the space surrounding the particles, the following homogeneous reaction occurs:



Waters et al.¹⁹ pointed out that the burning of CO surrounding carbon particles is very important. Reaction 4 is in equilibrium; the increase, for example, of the partial pressure of CO₂ may favor the production of CO instead of CO₂, in accordance with the Le Chatelier principle. Elayeb²⁰ used a three-equation model at the local scale to determine the local thermochemical conditions. These aspects will be important in the present paper.

In the sequel of the paper, the complex chemistry of carbon oxidation will be described using the very simple stoichiometric equation

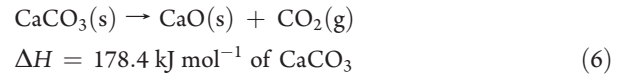


where frCO is the fraction of carbon oxidized to CO. This reaction results from an upscaled kinetic model at the Darcy scale obtained from the complex local reactive problem. Several attempts have been made in the past few years to understand the behavior of solid combustion (see for instance ref 21) or to determine, in two-dimensional (2D) geometries, some regimes and reduced kinetic models using a full microscopic model coupling heat and mass transfer.²⁰

1.4. Literature on Decarbonation of CaCO₃ and Carbonation of CaO. The decarbonation of CaCO₃ plays a major role in

the SC smoldering process because its high reaction heat impacts strongly the heat balance of the process and because it produces large amounts of CO₂. Moreover, CaO produced by this reaction may in turn undergo carbonation to CaCO₃. The latter reaction is strongly exothermic and consumes CO₂. A rapid overview of the state of the art in the decarbonation of CaCO₃ to CaO and the possible carbonation of CaO to CaCO₃ is proposed here to aid interpretation of the experimental results given in this paper.

1.4.1. Decarbonation. The decarbonation reaction of limestone is presented globally as follows:



This reaction, which has been studied extensively in the literature, has many aspects that are not well-understood. There is thus no consensus about several fundamental aspects, such as rate-limiting processes and the influence of CO₂ partial pressure on the reaction rate.

Predicting the behavior of a given limestone in a decarbonation process is difficult and involves large uncertainties. This is due to the complexity of the decarbonation process, which involves a five-step mechanism, according to Cheng and Specht:²² heat transfer to the solid surface of the particle, conduction of heat from the surface to the interior of the grain, the chemical reaction itself, diffusion of CO₂ to the surface, and then its discharge into the surrounding system.

Even for small particles, the process is thought to operate as a reacting front propagating from the particle surface to its center. Incidentally, such sharp front-like processes at the pore scale are difficult to describe in terms of macro-scale models. Three possible rate-limiting processes involved in the decomposition of carbonates can be distinguished inside the particle: (1) heat transfer through the particle to the reaction interface, (2) mass transfer of CO₂ released from the reaction surface through the porous system (pore diffusion), and (3) chemical reaction.²³ External mass transfer could also be a rate-limiting process in some cases. The relative importance of the different limiting steps on the observed reaction rate may be largely due to experimental conditions, experimental setup, and sample size.

The endothermic decarbonation reaction is favored by higher temperatures. It will proceed only if the partial pressure of CO₂ in the gas around the solid surface is less than the so-called decomposition pressure (or equilibrium pressure), which, in turn, is determined by considerations of equilibrium thermodynamics. A typical expression for equilibrium pressure in mmHg is given by²⁴

$$\log_{10} P_{\text{eq}} = -\frac{8792.3}{T(\text{K})} + 10.4022 \quad (7)$$

Figure 1 plots the phase diagram evolution of this equilibrium pressure in the temperature space. This figure shows that, for each temperature, there is a partial pressure of CO₂ at which a CaCO₃/CaO system does not undergo any reaction. If the CO₂ partial pressure is higher than the equilibrium pressure, evolution toward CaCO₃ is favored and inversely. At room temperature, the equilibrium overwhelmingly favors CaCO₃, because the equilibrium CO₂ pressure is only a tiny fraction of the partial CO₂ pressure in air (500 ppm). At temperatures above 650 °C, the CO₂ equilibrium pressure begins to exceed the CO₂ partial pressure in air (too small of a value to be plotted in Figure 1) and calcium carbonate begins to outgas CO₂ into air. The temperature at which limestone yields calcium oxide is usually given as ~825 °C. At this temperature,

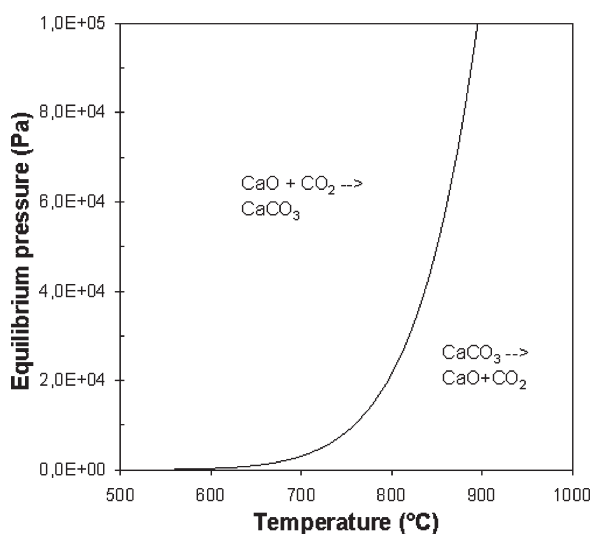
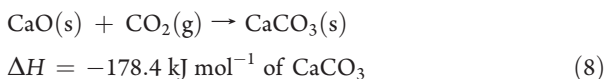


Figure 1. Equilibrium pressure for the CaCO_3 – CaO system

decarbonation will occur even under CO_2 partial pressures as high as 0.35 atm. If the partial pressure of CO_2 is higher than this equilibrium pressure, the carbonation to CaO is favored.

1.4.2. *Carbonation.* The carbonation reaction has been the object of numerous studies, in particular for CO_2 capture based on chemical looping processes. The use of CaO -based solids to capture CO_2 at high temperatures is at the core of several CO_2 -capture and zero-emission power plant concepts.^{25,26} These processes make use of the following reaction:



It is well-known that the solid–gas CaO – CO_2 reaction, considering one single particle, proceeds through two rate-controlling regimes. At the very initial stage of the reaction, the reaction occurs rapidly by heterogeneous surface chemical reaction kinetics. Following this initial stage, a compact layer of CaCO_3 is developed, inducing a progressive change in the reaction mechanism: the rate of the reaction decreases because of the diffusion limitation of reacting species through the layer.²⁷ From the viewpoint of the intrinsic CaO – CO_2 reaction, elevating CO_2 partial pressure should enhance the carbonation rate of CaO .

State of the art results show that the carbonation reaction kinetics for particles principally depends upon the experimental conditions. The rate of this reaction is affected by the temperature, CO_2 partial pressure, total pressure, and particle diameter. Literature dealing with the effect of the temperature and CO_2 partial pressure on this reaction will be cited in the discussion later in this paper.

1.4.3. *Present Investigation.* On the basis of this literature, CO_2 can be expected to have an impact in two co-occurring and positive ways: (i) an increase in CO production and a decrease in CO_2 production during carbon oxidation and (ii) the limitation of the extent of CaCO_3 decarbonation or the occurrence of some CaO carbonation, both leading globally to a reduction in CO_2 emissions.

An investigation was thus carried out using CO_2 -enriched air to feed the smoldering front. Reference cases were first established, in which air was used. The following smoldering front characteristics were observed: temperature, velocity, and produced

gas composition. Interest was more particularly focused on the fraction of CaCO_3 that was decarbonated and the yields in CO and CO_2 resulting from carbon oxidation. It was observed that adding CO_2 significantly impacted the two above-mentioned phenomena.

1.4.4. *Methodology.* All of the mechanisms involved in the process have been well-characterized in a previous work.²⁸ Quantitative results on the extent of each reaction were established by varying a number of parameters. The two following cases will be taken as references in this work. (i) First, a mixture of SC and sand was used, with an initial weight composition of 50%/50%. This led to contents of 3.5% mass of FC and 22.42% mass of CaCO_3 . The observed peak temperature was approximately 1032 °C. This experiment served as our base high-temperature test case. It was observed that the propagation of the smoldering front oxidized almost all FC, decarbonated all CaCO_3 mineral present in the medium, and consumed all supplied O_2 . The front velocity was equal to 4.04 mm min^{-1} . The value of the frCO parameter was about 0.31. This case corresponds to the classic situation where the smoldering front temperature is not controlled and results essentially from the carbon content of the medium and the amount of oxygen in the feed gas, usually air. The best known example is *in situ* combustion, where the smoldering front is generated on one side of the reservoir and is fed by injecting air. (ii) A second case, which represents the reference low-temperature test for this work, was obtained with less FC in the medium. The medium contains 2.08% mass of FC and 22.42% mass of CaCO_3 . The smoldering front propagates at 4.84 mm min^{-1} , and its peak temperature is 685 °C. Only 21.2% mass of the initially present CaCO_3 was decarbonated after the front passage. The stoichiometric parameter frCO was found to be equal to 0.21. This situation corresponds to *ex situ* applications, in which the medium composition can be controlled, allowing for a smoldering front temperature reduction.²⁸

New experiments were carried out in similar porous media but using CO_2 -enriched air to feed the front. It was decided to maintain O_2 at the same fraction as that of air in reference cases and in the so-called CO_2 -enriched air experiments to change only one parameter (CO_2 concentration) at a time. A molar fraction of 20% CO_2 was prepared. This value is high enough to expect an impact on the process and low enough for potential future applications, such as *in situ* oil recovery. We used a mixture of air, oxygen, and CO_2 , prepared using mass flow meter/controllers. Because of some uncertainties in the measured values and in the values identified using the mass balance, experiments were all repeated 2 or 3 times in each condition.

2. EXPERIMENTAL DEVICES AND PROCEDURES

The same porous medium was used as in the previous work²⁸ and for the same reasons. Performing experiments with SC instead of OS facilitates the interpretation of the results, because the LTO reactions and the devolatilization reaction no longer occur when SC is used. These two reactions are avoided in SC media because the only organic matter in the medium is FC, which only undergoes HTO. Furthermore, we prevent oil formation and, therefore, do not have to take it into account, which makes it possible to establish a proper mass balance.

2.1. *Preparation of SC and Characteristics.* The original OS sample used here is from the same batch as that used in refs 14, 15, and 28. It originates from the deposit of Timahdit in Morocco. It was received as hard dark-gray blocks, crushed using a rock-grinding device

Table 1. Proximate Analysis of the Original OS and the Prepared SC

component	proximate analysis (wt %)				
	H ₂ O	volatile matter	FC	CaCO ₃	inert
OS	2.5	14.7	4.70	34.6	43.5
SC		0.70	6.95	44.83	47.52

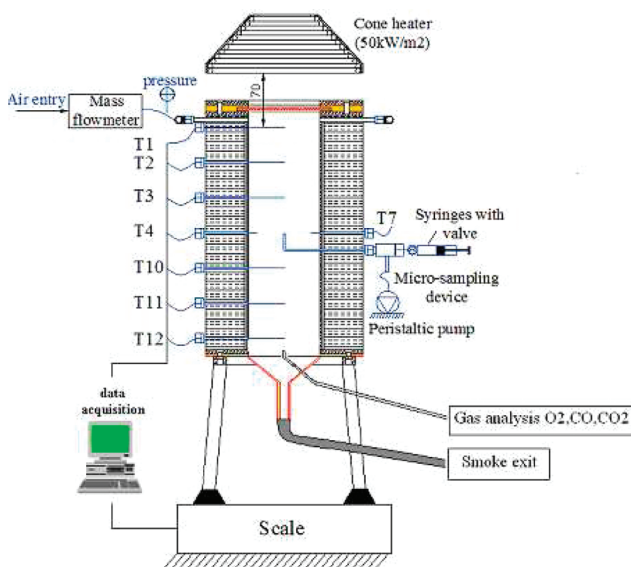


Figure 2. Cell combustion in porous medium, with continuous gas sampling at the axis.

and sieved to the experimental samples between 500 and 2000 μm . The SC was prepared by retorting OS at a pyrolysis temperature of 550 $^{\circ}\text{C}$ in a stainless-steel reactor externally heated by an electric rig furnace, in an atmospheric environment and using a heating rate of 5 $^{\circ}\text{C min}^{-1}$.

A horizontal tube furnace was used to characterize the initial OS, the prepared SC, and the solid residue after combustion. Details on the procedures can be found in ref 28. The proximate analysis for the initial OS and the prepared SC is shown in Table 1.

2.2. Combustion Cell. SC combustion experiments were performed with a fixed-bed reactor (Figure 2). A detailed description of this reactor was given in refs 14 and 28.

In all experiments, an oxidizer gas flow rate of 8.3 L min^{-1} at standard temperature and pressure (STP), which is equivalent to a Darcy velocity of 0.023 m s^{-1} at STP, is fed into the top of a vertical cylinder containing a mixture of crushed OS SC and inert sand. Ignition also takes place at the top of the sample using a cone heater that irradiates the surface through a quartz window.

During the experiment, temperatures in the bed were measured by six type-K thermocouples located along the axis of the cell at different heights (T1, T2, T3, T10, T11, and T12). The bed mass loss and pressure drop evolutions were recorded. Gas analyzers were connected to the sampling device at the axis of the cell, near the bottom, to analyze gases every 4 min, CO and CO₂ by gas chromatography and O₂ using a paramagnetic analyzer in a continuous mode.

To start a uniform front ignition across the whole surface of the bed, a cone radiant heater was used. A 1 cm layer of pure SC was put at the top of the bed to guarantee as far as possible a homogeneous ignition. The time of ignition was 300 s, with a radiative heat flux of 50 kW m^{-2} .

After each experiment, the mass evolution of the system, the temperature evolution of the thermocouples, and gas composition values were interpreted on the basis of a mass balance for the smoldering front. Three values were derived from these data: the fraction of FC oxidized to CO, frCO , the decarbonated fraction, $\text{fr}_{\text{decarb}}$, and the smoldering front velocity, ν_{fr} . Details of the mass balance equations and the parameter identification procedure are given in ref 28.

The mass balance from which the values of ν_{fr} , frCO , and $\text{fr}_{\text{decarb}}$ are derived was established as the front was located approximately two-thirds away from the top of the cell. In this zone, the front was observed to propagate at a constant velocity; both the gas species fractions in the flue gas and the cell mass loss rate were constant along time. It is believed that buoyancy did not produce a significant effect at this time thanks to the 100 mm high zone remaining downstream of the front.

3. RESULTS AND INTERPRETATIONS

The results for all experiments, before any calculation from a mass balance, are reported in Table 2.

3.1. At High Temperatures. Let us first examine results obtained with the medium containing 3.47% FC conditions, which lead to a high-temperature front.

The front temperature slightly decreased with CO₂ addition, from an average of 1032 to 957 $^{\circ}\text{C}$. All of the feed oxygen was still consumed, as in the reference case. Analyzing the solid residue after combustion indicated that the amount of remaining FC was less than 0.25%, as observed in the reference case. The fraction of CO in the flue gas had significantly increased, from 5.4% in the reference case to 8.9% in the CO₂-enriched experiment. Because CO was the only fuel gas in the flue gas, the calorific value increased in the same proportion. It is clear that more CO had been produced during FC oxidation, but this increase in the molar fraction may also have been due to a decrease in the total produced gas flow rate, if less CaCO₃ was decarbonated. The produced CO₂ fraction, which is equal to 25.4% in the reference case, decreased to 42.6 – 20 (injected) \approx 22.6%. Nevertheless, because CO₂ results from both FC oxidation and CaCO₃ decarbonation, this cannot be interpreted directly.

The parameters frCO and $\text{fr}_{\text{decarb}}$ were then determined for better interpretation of the experiments. A parameter identification procedure was employed using a mass balance as the direct model. Results, which are reported at the bottom of Table 2, are interpreted below.

3.1.1. Impact of CO₂-Enriched Gas on Decarbonation. Figure 3 plots the decarbonated fraction as a function of the smoldering front temperature. The decarbonation fraction decreased on average values from 98 to 68% when feeding the smoldering front with CO₂-enriched air. This is an important result from this work: 30% of the decarbonation of the carbonates can be avoided by adding 20% CO₂ to the feed gas. This may find applications in both *in situ* or *ex situ* contexts.

A first possible explanation is that the presence of CO₂ in the feed air influenced the decarbonation reaction. In the literature, a large number of expressions of the decarbonation rate as a function of the CO₂ partial pressure (or CO₂ concentration) are proposed. A sharp decrease in the decarbonation rate was found at the highest CO₂ concentrations.²³ Ingraham and Marier²⁹ found that the reaction rate linearly depended upon the difference between the CO₂ partial pressure at the reaction surface and the equilibrium pressure. Following the same idea, Khinast et al.³⁰ found an exponential decay in the reaction rate constant with the CO₂ partial pressure. Hashimoto³¹ reported that the rate dependency upon CO₂ partial pressure was linear at lower temperatures

Table 2. Synthesis of the Experimental Results

		(a) High-Temperature Case					
		high-temperature FC = 3.47 mass %					
		air (reference)			CO ₂ -enriched air		
raw results	front temperature (°C)	1037	1004	1056	918	950.5	1003
	residual O ₂ (vol %)	<0.05	<0.05	<0.05	<0.05	<0.05	<0.05
	CO (vol %)	5.38	4.94	5.95	6.98	9.12	10.6
	CO ₂ (vol %)	25.9	25.6	24.9	42.4	41.2	43.5
identified parameters	ν_{frC}	4.02	4.03	4.07	4.43	4.57	4.7
	frCO	0.32	0.29	0.34	0.35	0.43	0.44
	fr _{decarb}	1.065	0.937	0.952	0.71	0.72	0.6

		(b) Low-Temperature Case					
		low-temperature FC = 2.09 mass %					
		air (reference)			CO ₂ -enriched air		
raw results	front temperature (°C)	727	685	685	685	733	
	residual O ₂ (vol %)	<0.05		4.72	3.16	0.82	
	CO (vol %)	3.22		2.85	3.21	3.83	
	CO ₂ (vol %)	14.5		14.4	36.0	41.1	
identified parameters	ν_{frC}	5.82		4.84	4.66	5.85	
	frCO	0.22		0.22	0.16	0.16	
	fr _{decarb}	0.14		0.2	0.001	0.021	

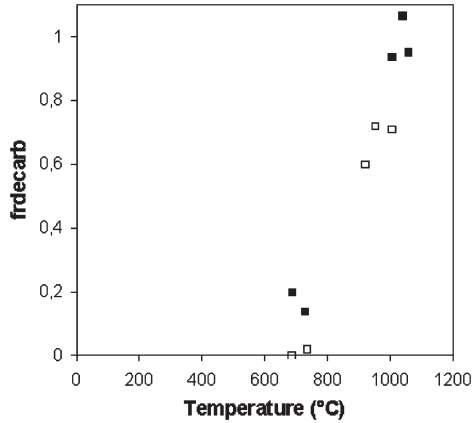


Figure 3. Decarbonated fraction versus the front temperature: (■) reference experiments and (□) experiments with CO₂-enriched air.

and nonlinear at higher temperatures. Rao et al.²⁴ also found a nonlinear dependency at 953–1148 K, with the degree of non-linearity dependent upon the temperature. Searcy and Darroudi³² found that, at low CO₂ partial pressures, the decarbonation rate was essentially independent of the partial pressure, whereas at higher values, there was a parabolic dependency, which changed to linear for values near the thermodynamic equilibrium. However, Huckauf et al.³³ mentioned that the reaction rate was inversely proportional to the difference between the CO₂ partial pressure and the equilibrium pressure.

To summarize, the reaction at the CaCO₃–CaO interface is complex, not fully understood, and related to the CO₂ partial pressure in the surrounding gas. However, to evaluate the potential impact of increasing the CO₂ partial pressure on the decarbonation reaction around 950 °C, we consider here the

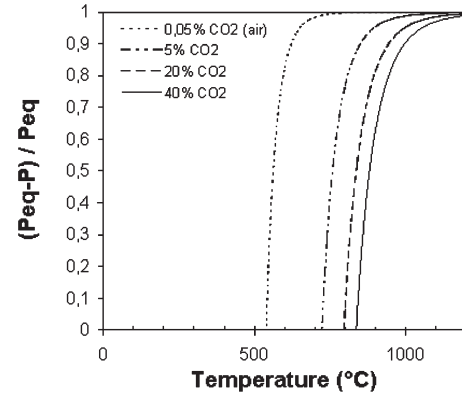


Figure 4. Ratio $(P_{\text{eq}} - P)/P_{\text{eq}}$ versus the temperature for different CO₂ pressures.

classic model of ref 34 that expresses the decarbonation rate as proportional to

$$R_d = K_d \frac{P_{\text{eq}} - P}{P_{\text{eq}}} \quad (9)$$

where R_d is the rate of decarbonation, K_d is the rate coefficient, and P is the partial pressure of CO₂. We have plotted in Figure 4 the term $(P_{\text{eq}} - P)/P_{\text{eq}}$ versus the temperature, for different values of the ambient partial pressure of CO₂.

At 950 °C, the term $(P_{\text{eq}} - P)/P_{\text{eq}}$ is equal to 1 under air, corresponding to the situation where the decarbonation occurs at the maximum rate. Martins et al.¹⁴ have shown that the zone where the decarbonation occurs is superposed on the zone where carbon oxidation occurs. Therefore, during the reference case, the CO₂ partial pressure in the reaction zone may vary between

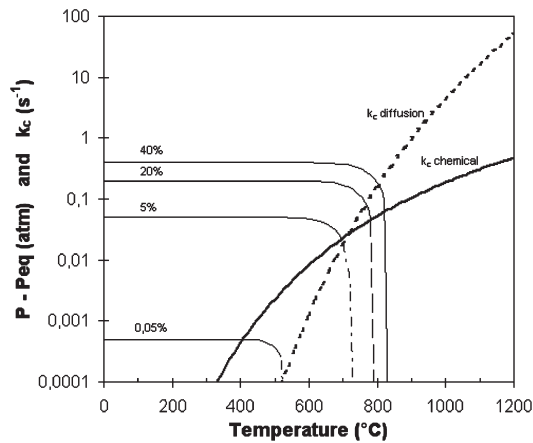


Figure 5. Value for the term $P_{\text{eq}} - P$ at different CO_2 partial pressures and the rate coefficient k_c ³⁶ appearing in the expression of the reaction rate for CaO carbonation at different pressures of CO_2 .

0.05 (in air) and 25%, as measured at the exit of the cell, whereas in CO_2 -enriched air experiments, it varies between 20 (feed gas) and 42.6%, as measured at the exit of the cell.

Taking 900 °C as the average temperature for the decarbonation zone, Figure 4 indicates that the increase in the partial pressure of CO_2 to 20 or 40% involves the decrease in of the term $(P_{\text{eq}} - P)/P_{\text{eq}}$ from 1 to 0.8 and 0.6, respectively; decarbonation is slowed in the same ratio. It is clear that the quantitative values determined here should not be considered because of the uncertainty remaining in the calculation of the $(P_{\text{eq}} - P)/P_{\text{eq}}$ term, which is strongly dependent upon the temperature. Nevertheless, this simple modeling indicates that an increase in the CO_2 partial pressure by 20% can impact significantly and slow decarbonation. This is the probable explanation for the decrease in the progress of decarbonation from 98 to 68%, observed experimentally when adding 20% CO_2 in the feed gas.

Another possible explanation could be that some carbonation of CaO to CaCO_3 occurred, leading to finally observed lower decarbonation degrees. From the literature, elevating the CO_2 partial pressure may enhance the carbonation rate of CaO. Oakson and Cutler³⁵ considered that the carbonation rate was a function of the CO_2 partial pressure and temperature based on the carbonation at 850–1044 °C with a CO_2 partial pressure of 245–2487 kPa. Bhatia and Perlmutter³⁶ found that the initial fast carbonation reaction correlated with reversible first-order kinetics when the carbonation was conducted at 400–725 °C with a CO_2 partial pressure of 10–42 kPa. Later, Grasa et al.³⁷ conducted the cyclic carbonation at 650 °C for 20 min by varying the CO_2 partial pressure from 0.002 to 0.1 MPa and found that the fast carbonation reaction period was strongly affected by the concentration of the reactant during the multiple cycles. The first-order reaction of CaO with respect to CO_2 was verified, consistent with the results from ref 36. Sun et al.³⁸ detected a variable order reaction of CaO with respect to the CO_2 partial pressure, from the first-order reaction to the zero-order dependence when the CO_2 partial pressure exceeded ~ 10 kPa.

Finally, the works from the literature reflect the fact that the multi-scale elementary mechanisms involved in the CaO carbonation process are not well-understood. To support interpretation of the present results, the works of Bhatia and Perlmutter³⁶ will be used. These authors distinguished the chemical control

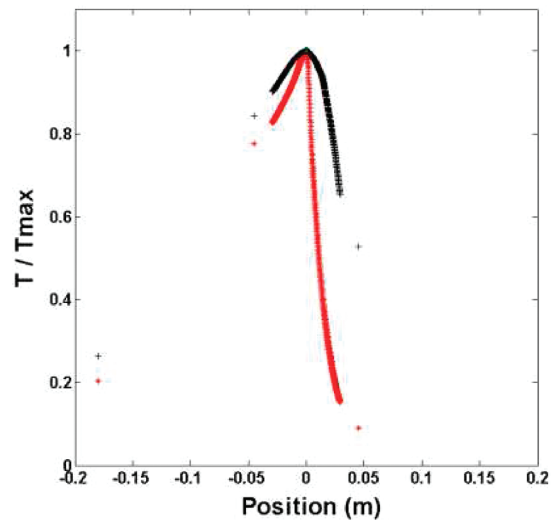


Figure 6. Temperature profile around the peak temperature in the (*) reference case and (+) CO_2 -enriched air experiment.

regime and the diffusional control regime; the carbonation reaction rate can be expressed as

$$R_c = k_c(P_{\text{eq}} - P) \quad (10)$$

where R_c is the rate of carbonation, k_c is the rate coefficient, and P is the partial pressure of CO_2 . Figure 5 gives the rate coefficient of the carbonation reaction in both regimes versus the temperature, according to these authors. The term that appears in the expression of the reaction rate was also plotted on this figure for several values of the CO_2 partial pressure between 0.05 (air) and 40%.

The figure shows that the term is positive only for temperatures lower than 800 °C, regardless of the CO_2 partial pressure between 5 and 40%. Carbonation may occur only in the front zone corresponding to these temperatures. At 700 °C, for instance, the results show that an increase in the CO_2 partial pressure (P) from 5 to 20% results in an increase by 1 decade of the term $P_{\text{eq}} - P$, and, consequently, of the carbonation kinetics. Around this temperature, both the term $P_{\text{eq}} - P$ and k_c may vary in the range from 10^{-2} to 10^{-1} , leading to a product between 10^{-4} and 10^{-2} s^{-1} . Considering the value of 10^{-2} s^{-1} , some carbonation may occur because the medium remains at such temperatures for several minutes, while for the value of 10^{-4} s^{-1} , carbonation is not likely to occur because it is too slow. Therefore, it is difficult, given the uncertainties in the values for the kinetic parameters in the literature, to establish whether carbonation may occur or not.

With regard to the present experimental results, it is also very difficult to verify if carbonation took place or not. When the temperature curve shape in the reference case is compared to the experiment with CO_2 as shown in Figure 6, we observe that the peak becomes wider by adding CO_2 . This may be explained by the fact that some carbonation (an exothermic reaction) occurs just downstream of the decarbonation reaction, which leads to a temperature rise and, hence, this peak shape. Nevertheless, the lack of experimental evidence does not enable us to conclude on this point. The difference in the peak shape was nevertheless systematically observed and confirms the impact of CO_2 -enriched air on the smoldering process.

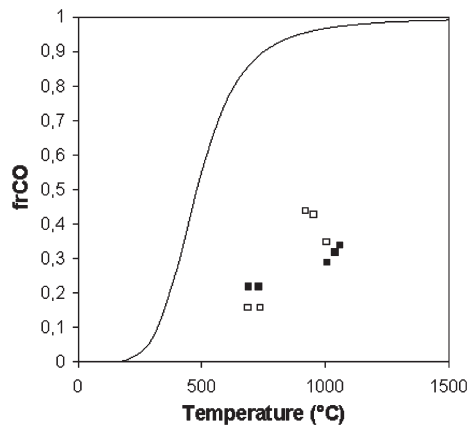


Figure 7. Fraction of carbon oxidized to CO versus the front temperature: (—) theoretical evolution, (■) reference experiments, and (□) experiments with CO₂-enriched air.

3.1.2. *Impact of CO₂-Enriched Gas on Carbon Oxidation.* Figure 7 plots the fraction of carbon oxidized to CO (fr_{CO}) as a function of the peak temperature. At high temperatures, the fr_{CO} increases from 0.3 on average in the reference case to 0.4 when adding 20% CO₂ to the incoming air. This result is very interesting in two ways: (i) The produced gas contains more CO, which increases its calorific value. (ii) An increase of fr_{CO} theoretically induces a decrease in the temperature of the front²⁸ and, thus, favors a decrease in the decarbonation rate.

In the literature, it is generally observed that oxidation of char releases predominantly CO₂ at relatively lower temperatures. As the temperature increases, more CO is produced, while CO₂ diminishes sharply. The Arrhenius-type equation is usually employed to describe the effect of the temperature on the ratio CO/CO₂. Several expressions have been given in the literature.^{39,40} Other authors studied the effect of the partial pressure of oxygen and temperature on CO/CO₂ and obtained expressions as functions of these two parameters.^{18,41} Monson et al.⁴² have conducted experiments in char combustion at atmospheric and elevated pressures. They suggest an exponential correlation for the ratio CO/CO₂, in which the product of surface reactions is predominantly carbon dioxide at temperatures lower than 1500 K; the ratio equals 1 when the reaction temperature is about 1700 K. To illustrate this, we have plotted in Figure 7 the evolution of fr_{CO} according to ref 39. Large differences exist between this curve and the present experimental results, which may be explained by numerous factors, as discussed above. Nevertheless, the fr_{CO} evolution with temperature observed in this work remains compatible with the literature.

The addition of CO₂ provokes a change in the partial pressure of CO₂ in the surrounding gas of the medium particles. This change may shift the equilibrium of some reactions, according to the Le Chatelier principle. Among these reactions, the oxidation of CO into CO₂ (reaction 4), which takes place in the space surrounding the particles likely to be impacted, and the increase in the partial pressure of CO₂ may have favored the carbon oxidation reaction toward the production of CO.

Some elements of interpretation can be found by observing Figure 8. This figure plots the theoretical and experimental values of the front velocities versus fr_{CO} . When experiments at high temperatures are considered (around the bottom curve), the average values obtained show that adding CO₂ causes a noteworthy

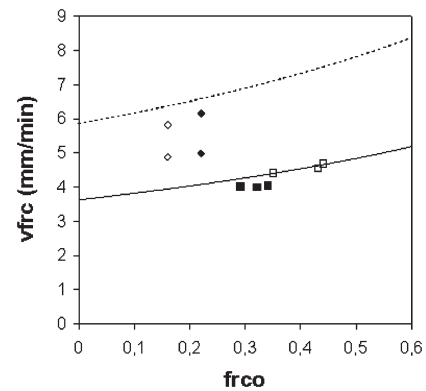


Figure 8. Front velocity versus the fraction of carbon oxidized to CO: (■) reference experiments, (□) experiments with CO₂-enriched gas, (—) theoretical value for high-temperature experiments (3.47% FC), and (---) theoretical value for low-temperature experiments (2.09% FC).

increase in the front velocity from 4.04 to 4.56 mm min⁻¹. The theoretical velocity was calculated by stoichiometric calculations for the carbon oxidation reaction following equation 5, taking into account the fact that all FC is oxidized and assuming that all of the feed O₂ is consumed. At high temperatures, a very good agreement between theoretical and experimental values of front velocity is obtained. This attests to the quality of measurements and the parameter identification procedure for fr_{CO} , fr_{decarb} , and v_{frC} . The experimental front acceleration is in agreement with the fact that fr_{CO} increases.

At this stage, it is possible to discuss further the fact that the front temperature appeared unchanged when adding CO₂ to the feed air. With reference to an energy balance as detailed in ref 28, the decrease in the decarbonation degree from 98 to 68% theoretically induces a front temperature increase of 225 °C. On the other hand, the increase of fr_{CO} from 0.32 to 0.41 theoretically induces a front temperature decrease of 235 °C. It is known from the literature that a thermal balance gives poor estimates of the front temperature. Our previous work nevertheless indicated reasonable prediction. Therefore, it is thought that the apparently unchanged front temperature observed here is the result of two antagonist impacts that occurred simultaneously.

3.2. *At Low Temperatures.* Let us now consider the results obtained at low temperatures, using a solid medium containing 2.08% FC. The front temperature remained around 700 °C with CO₂ addition, as in the reference case (Table 2). The amount of oxygen in the flue gas varied when repeating this experiment (Table 2), which is explained by instability of the front at low temperatures. Oxygen is only partially consumed: on average, 1.0% O₂ is found in the produced gas in the experiments with CO₂-enriched air, while 2.4% O₂ was present in the reference cases.

A slight increase of the CO concentration in the produced gas was observed, from an average of 3.03 to 3.52%. Produced CO₂, which was equal to 14.4% in the reference cases, increased slightly to 38.5 – 20 ≈ 18.5%. The values of fr_{CO} , fr_{decarb} , and v_{frC} were derived again from the parameter identification procedure and enable further interpretation, as discussed below.

3.2.1. *Impact of CO₂-Enriched Gas on Decarbonation.* The values of the decarbonated fraction at low temperatures are also reported in Table 2 and plotted in Figure 3. The decarbonated fraction decreased from 21% in the reference case to about 0% by adding CO₂. The decarbonation reaction was totally suppressed. This is one of the major results of this work, because it demonstrates

that combining fuel preparation by mixing with an inert medium and enriching the feed gas into CO₂ causes full oxidation of the FC in SC without inducing any decarbonation of the medium.

The first element of interpretation can be found by returning to Figure 4. Under air, the term $(P_{\text{eq}} - P)/P_{\text{eq}}$ is equal to 1 at the temperature ~ 700 °C and the decarbonation operates at maximum velocity. When the partial pressure of CO₂ increases to 20 or 40%, the term $(P_{\text{eq}} - P)/P_{\text{eq}}$ becomes negative; the decarbonation reaction is stopped. This shows that the presence of CO₂ in larger amounts during experiments with CO₂-enriched gas is very likely responsible for the non-decarbonation of CaCO₃.

With regard to the possible occurrence of some carbonation of CaO back to CaCO₃, the same approach as that used for high-temperature experiments can be considered. However, it remains impossible here to establish whether CaO carbonation did occur or not.

3.2.2. *Impact of CO₂-Enriched Air on Carbon Oxidation.* An analysis of experiments at low temperatures shown in Figure 7 reveals that the CO₂-enriched air affected frCO in the opposite way compared to experiments at high temperatures. Here, the addition of CO₂ in the feed air led to a slight decrease in frCO. No explanation can be found for this decrease. Returning to Figure 8, some elements can be confirmed. Considering the theoretical front velocity (dashed line) and the experimental results (4 points at the top of the figure), it can be seen that, for two experiments, the values are close to the theoretical values. For these two experiments, the remaining oxygen in the flue gas was at <0.05 and 0.82%, indicating that all of the feed O₂ was consumed. This explains that the mass balance theory is almost satisfied. The two points further from theory correspond to experiments where 4.72 and 3.16% O₂ were left in the flue gas, which explains the experimentally observed slowing of the front.

4. CONCLUSION

The effect of adding CO₂ to the oxidizer air feeding the smoldering front in OS SC porous medium was experimentally investigated. The effect of CO₂ on the decarbonation of carbonates and the carbon oxidation reaction, which represent the main reactions for such smoldering processes, were investigated quantitatively.

At high temperatures, illustrating a situation where the front temperature is not controlled (*in situ* combustion, for example), adding 20% CO₂ limits the decarbonated fraction at 68%, instead of 98% when using air. The production of CO during FC oxidation increases by about 40%. Together with the decrease in the progress of decarbonation, this results in an increase in the CO fraction in the flue gas from 5.4 to 8.9%.

The calorific value of the flue gas increases in the same proportion. The velocity of the front increased from 4.04 to 4.56 mm min⁻¹ (12%). This confirms the control of the front velocity by FC oxidation stoichiometry and corresponds quantitatively with the rise in CO production.

The front temperature appears to be unchanged, but it is strongly suggested that this resulted from two antagonistic phenomena: the decrease in the decarbonated fraction would increase the temperature, while the increase in the fraction of FC oxidized to CO (frCO) would decrease this temperature.

At low temperatures, illustrating a situation where the front temperature is controlled by fuel dilution with an inert medium

(such as in *ex situ* combustion), the decarbonation reaction was totally suppressed.

It is thought that, in both cases, the reason for lower global decarbonation is the slowing of the decarbonation reaction because of the increase in the CO₂ partial pressure. Evidence is lacking to establish whether CaO carbonation occurs or not. It is shown that adding 20% CO₂ to the feed air affects the temperature profile around the peak temperature, leading to a larger and smoother shape.

■ AUTHOR INFORMATION

Corresponding Author

*E-mail: mohamed.sennoune@mines-albi.fr.

■ ACKNOWLEDGMENT

The authors are most grateful to Bernard Auduc for his technical support during all experiments.

■ REFERENCES

- (1) Akkutlu, I.; Yortsos, Y. *Combust. Flame* **2003**, *134*, 229–247.
- (2) Mailybaev, A.; Bruining, J.; Marchesin, D. *Combust. Flame* **2011**, *158*, 1097–1108.
- (3) Vantelon, J.; Lodeho, B.; Pignoux, S.; Ellzey, J.; Torero, J. *Proc. Combust. Inst.* **2005**, *30*, 2239–2246.
- (4) Pironi, P.; Switzer, C.; Rein, G.; Fuentes, A.; Gerhard, J.; Torero, J. *Proc. Combust. Inst.* **2009**, *32*, 1957–1964.
- (5) Rein, G.; Cleaver, N.; Ashton, C.; Pironi, P.; Torero, J. *Catena* **2008**, *74*, 304–309.
- (6) Page, S.; Siegert, F.; Rieley, J.; Boehm, H.; Jaya, A.; Limin, S. *Nature* **2002**, *420*, 61–65.
- (7) Ohlemiller, T. *Prog. Energy Combust. Sci.* **1985**, *11*, 277–310.
- (8) Howell, J.; Hall, M.; Ellzey, J. *Prog. Energy Combust. Sci.* **1996**, *22*, 121–145.
- (9) Kahru, A.; Pöllumaa, L. *Oil Shale* **2006**, *23*, 53–93.
- (10) Jiang, X.; Han, X.; Cui, Z. *Prog. Energy Combust. Sci.* **2007**, *33*, 552–579.
- (11) Han, X.; Jiang, X.; Cui, Z. *J. Therm. Anal. Calorim.* **2008**, *92*, 595–600.
- (12) Uibu, M.; Uus, M.; Kuusik, R. *J. Environ. Manage.* **2009**, *90*, 1253–1260.
- (13) Kulaots, I.; Goldfarb, J.; Suuberg, E. *Fuel* **2010**, *89*, 3300–3306.
- (14) Martins, M.; Salvador, S.; Thovert, J.; Debenest, G. *Fuel* **2010**, *89*, 133–143.
- (15) Martins, M.; Salvador, S.; Thovert, J.; Debenest, G. *Fuel* **2010**, *89*, 144–151.
- (16) Fennell, P.; Kadchha, S.; Lee, H.; Dennis, J.; Hayhurst, A. *Chem. Eng. Sci.* **2007**, *62*, 608–618.
- (17) Laurendeau, N. *Prog. Energy Combust. Sci.* **1978**, *4*, 221–270.
- (18) Smith, I. *Symp. (Int.) Combust., [Proc.]* **1982**, *19*, 1045–1065.
- (19) Waters, B.; Squires, R.; Laurendeau, N.; Mitchell, R. *Combust. Flame* **1988**, *74*, 91–106.
- (20) Elayeb, M. Modélisation à l'échelle microscopique de transports avec réaction en milieu poreux: Combustion en lit fixe. Ph.D. Thesis, Université de Poitiers, Poitiers, France, 2008.
- (21) Debenest, G.; Mourzenko, V.; Thovert, J. *Combust. Theory Modell.* **2005**, *9*, 113–135.
- (22) Cheng, C.; Specht, E. *Thermochim. Acta* **2006**, *449*, 8–15.
- (23) Garcia-Labiano, F.; Abad, A.; De Diego, L.; Gayán, P.; Adánez, J. *Chem. Eng. Sci.* **2002**, *57*, 2381–2393.
- (24) Rao, T.; Gunn, D.; Bowen, J. *Chem. Eng. Res. Des.* **1989**, *67*, 38–47.
- (25) Anthony, E. *Ind. Eng. Chem. Res.* **2008**, *47*, 1747–1754.
- (26) Harrison, D. *Ind. Eng. Chem. Res.* **2008**, *47*, 6486–6501.
- (27) Nikulshina, V.; Gálvez, M. E.; Steinfeld, A. *Chem. Eng. J.* **2007**, *129*, 75–83.

- (28) Sennoune, M.; Salvador, S.; Quintard, M. *Combust. Flame* **2011**, *158*, 2272–2282.
- (29) Ingraham, T.; Marier, P. *Can. J. Chem. Eng.* **1963**, *41*, 170–173.
- (30) Khinast, J.; Krammer, G.; Brunner, C.; Staudinger, G. *Chem. Eng. Sci.* **1996**, *51*, 623–634.
- (31) Hashimoto, H. *J. Chem. Soc. Jpn.* **1962**, *64*, 1162–1165.
- (32) Searcy, A.; Darroudi, T. *J. Phys. Chem.* **1981**, *85*, 3971–3974.
- (33) Seidel, G.; Huckauf, H.; Starck, J.; Kerchove, P.; Chassard, A. *Technologie des Ciments, Chaux, Plâtres: Processus et Installations de Cuisson*; Septima: Paris, France, 1980.
- (34) Silcox, G.; Kramlich, J.; Pershing, D. *Ind. Eng. Chem. Res.* **1989**, *28*, 155–160.
- (35) Oakeson, W. G.; Cutler, I. B. *J. Am. Ceram. Soc.* **1979**, *62*, 556–558.
- (36) Bhatia, S.; Perlmutter, D. *AIChE J.* **1983**, *29*, 79–86.
- (37) Grasa, G.; Abanades, J.; Alonso, M.; González, B. *Chem. Eng. J.* **2008**, *137*, 561–567.
- (38) Sun, P.; Grace, J.; Lim, C.; Anthony, E. *Chem. Eng. Sci.* **2008**, *63*, 47–56.
- (39) Arthur, J. *Trans. Faraday Soc.* **1951**, *47*, 164–178.
- (40) Rossberg, M. *Electrochemistry* **1956**, *60*, 952.
- (41) Tognotti, L.; Longwell, J.; Sarofim, A. *Symp. (Int.) Combust., [Proc.]* **1991**, *23*, 1207–1213.
- (42) Monson, C.; Germane, G.; Blackham, A.; Douglas Smoot, L. *Combust. Flame* **1995**, *100*, 669–683.